Commensurability of the Spin-Density-Wave State of $(TMTSF)_2PF_6$ Observed by ^{13}C-NMR

Sanato Nagata, Masaki Misawa, Yoshihiko Ihara, and Atsushi Kawamoto*

Department of Condensed Matter Physics, Hokkaido University, Kita-ku, Sapporo, Hokkaido 060-0810, Japan

(Received 20 January 2013; published 15 April 2013)

A spin-density-wave (SDW) for $(TMTSF)_2PF_6$ has been reported to appear below T_{SDW} ($\simeq$ 12 K), with a subphase transition at T^* ($\simeq$ 4 K). To determine the structure of the subphase, we synthesized $(TMTSF)_2PF_6$, in which one side of the central carbon bond in each TMTSF molecule was replaced by ^{13}C, and utilized this compound in ^{13}C nuclear magnetic resonance measurements. Below T_{SDW}, the spectrum became broad and T_1^{-1} decreased, in agreement with previous results. Below T^*, fine structures emerged in the center of the spectrum and T_1^{-1} decreased exponentially. These phenomena were attributed to the emergence of commensurability at T^*.

DOI: 10.1103/PhysRevLett.110.167001 PACS numbers: 74.70.Kn, 75.30.Fv, 76.60.−k

$(TMTCF)_2X$ (C = S : TMTTF, tetra-methyl-tetra-thiafulvalene, C = Se : TMTSF, tetra-methyl-tetra-selenafulvalene) salts, in which X^- is a monovalent inorganic anion, are quasi-one-dimensional organic conductors [1]. The donor molecules of TMTCF form a one-dimensional stacked column, with weak intercolumn interactions [2]. These salts show the physical properties of a charge-ordered state, a spin-density-wave (SDW) state, and a superconductor state, with these properties controlled by pressure and chemical substitutions. $(TMTSF)_2X$, the so-called Bechgarrd salt, is the first known organic superconductor [3]. The dependence of the physical properties of these salts on physical and chemical pressure was summarized in a universal phase diagram [1]. In the high-pressure region, superconductivity lies adjacent to the SDW phase. In $(TMTSF)_2PF_6$, the SDW transition at ambient pressure is observed at 12.5 K, with superconductivity emerging at 1.6 K under a critical pressure of 0.65 $\sim$ 1 GPa [3]. Many theoretical and experimental studies on superconductivity and SDW states in $(TMTSF)_2X$ have been performed over the past three decades. Moreover, phenomena characteristic of a quasi-one-dimensional electron system have been observed, including a field-induced SDW state with the field perpendicular to the conducting plane [4].

The most important characteristic feature of this compound is its local magnetization at molecular sites. The amplitude of the SDW moment was estimated to be 0.08 μ_B/molecule by proton nuclear magnetic resonance (^1H NMR) [5] and 0.06 μ_B/electron (0.03 μ_B/molecule) by carbon nuclear magnetic resonance (^{13}C NMR) [6]. However the subphase below $T^* = 4$ K in the SDW phase has not been determined [5,7–10]. The spin-lattice-relaxation rate T_1^{-1}, determined by ^{77}Se NMR [7,11], ^{13}C NMR [6], and ^1H NMR [5,12], diverged at T_{SDW} and showed weak temperature dependence below T_{SDW}. Furthermore, T_1^{-1} in ^{77}Se NMR below T^* decreased exponentially, with $T_1^{-1} \propto \exp(-\Delta/k_BT)$. The existence of a Fermi surface at temperatures $T^* < T < T_{SDW}$ may be due to imperfect nesting, with the complete SDW state appearing below T^* [7]. In contrast, the specific heat of $(TMTSF)_2PF_6$ was also reported to be anomalous at T^* [10]. A glassy transition may explain many phenomena that occur around T^* [10]. The development of SDW domains with phase homogeneity was suggested by the temperature dependence of electric permittivity at several fixed frequencies below T^* [13]. The nonlinear electrical conductivity of $(TMTSF)_2ClO_4$ indicates an anomaly of residual carriers at T^* [9]. These results may be explained by a discommensurate structure below T^* to model the subphase [14,15], which was first investigated in TaS_3 [16]. Although thermodynamic measurements showed glass transition at around T^* [10], the details of the glassy state remain unclear.

Shubnikov—de Haas oscillations corresponding to magnetic breakdown orbits have been observed at magnetoresistances below the SDW transition above 15 T [17–19]. The oscillations abruptly vanish between 4.2 and 3.8 K [18] or below 2.5 K [19]. The mechanism of the disappearance is proposed to be an open Fermi surface [17,18] or some change of the nesting vector [19]. However, the mechanism has not been determined.

We utilized NMR spectra to reveal the structure of the subphase. In ^1H NMR, however, the spectrum did not change significantly due to the small hyperfine coupling constant and the large dipole interaction between the ^1H nuclei [5]. Although the hyperfine coupling constant was large in ^{77}Se NMR, four crystallographically independent ^{77}Se sites are present in each unit cell, and the broad spectrum of ^{77}Se signals complicates the analysis of these spectra. We therefore utilized site-selective ^{13}C NMR. Stochastic substitution of ^{13}C in 10% of the central double-bonded carbon sites has been used to assess the spectrum and T_1^{-1} above 4.2 K [6]. To clarify the structure of the subphase and related problems, we performed site-selective ^{13}C NMR on a sample in which 100% of the C sites on one side of the central C = C bonds were replaced by ^{13}C nuclei.

Single-site ^{13}C-enriched TMTSF was synthesized as described [20,21]. $(TMTSF)_2PF_6$ was prepared by a

 © 2013 American Physical Society

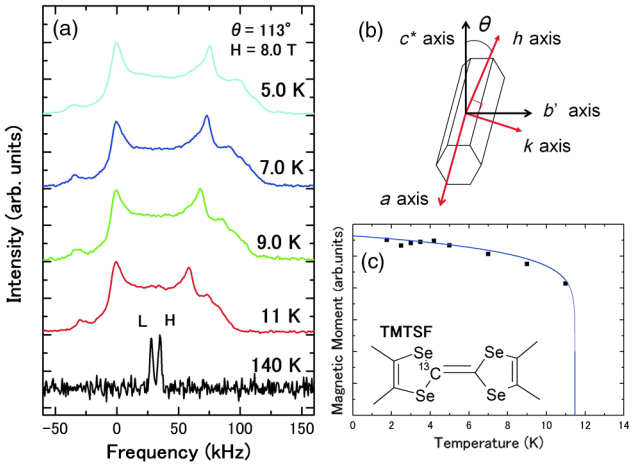

FIG. 1 (color online). (a) Temperature dependence of the NMR spectrum from 140 to 5 K with the magnetic field along the direction rotated 23° from the b' axis ($\theta = 113°$). (b) Crystal shape and (a, b', c^*) and (a, k, h) axes defined by us. (c) Temperature dependence of the moment of the SDW state. Inset: Isotope substituted TMTSF molecule.

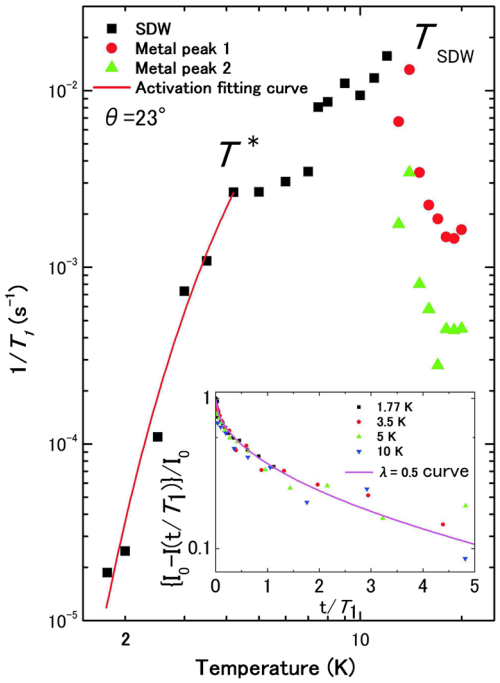

FIG. 2 (color online). Temperature dependence of T_1^{-1} in a magnetic field 23° from the c^* axis ($\theta = 23°$). Inset: Nuclear relaxation curves below T_{SDW}.

conventional electrochemical method. NMR measurements were performed at decreasing temperature under an 8.0 T field corresponding to the resonance frequency of 85.64 MHz. The h axis was set parallel to the external field and the angle of the field (h axis) from the c^* axis was defined as θ in the $c^* - b'$ plane; the k axis was parallel to the $h \times a$ direction [Fig. 1(b), in which b' corresponds to the $c^* \times a$ direction]. Spectra were obtained by fast Fourier transformation of the echo signal with a $\pi/2$-π pulse sequence. The typical $\pi/2$ pulse, $t_{\pi/2}$, was set at 3 μ sec. These widths correspond to the spectral range $1/(10t_{\pi/2})$, which was equivalent to ± 30 kHz. To cover the wide spectrum width of 160 kHz in the SDW state, we changed the resonance frequency every 50 kHz and calculated the average of these spectra. The spin-lattice relaxation time was measured by the saturation recovery method.

Figure 1(a) shows the temperature dependence of the NMR spectrum from 140 to 5 K at $\theta = 113°$. The two peaks (denoted H and L) in the metallic state correspond to the two crystallographically independent ^{13}C sites. We also observed a U-shaped incommensurate (IC) SDW spectrum of two independent ^{13}C sites below $T = 12$ K [Fig. 1(a)], similar to previously reported spectra. Figure 1(c) shows the temperature dependence of the amplitude $M(T)$. Fitting with $M(T) \propto [1 - (T/T_{SDW})]^{\beta}$ resulted in a β of 0.11.

Our main purpose was to study the behavior of this compound below T^*.T^* is notably observed with T_1^{-1}. To cover the NMR spectrum using a single rf frequency, we measured T_1^{-1} in a magnetic field parallel to the direction in which the width of the spectrum was narrow in the SDW state. Figure 2 shows the temperature dependence of T_1^{-1} in a magnetic field along the directions rotated 23° from the c^* axis ($\theta = 23°$). In contrast to the T_1^{-1} of the two peaks above T_{SDW}, which were well fitted by a single exponential function, the relaxation profiles below T_{SDW} could be fit by the equation $I(t) = I_0(1 - e^{-(t/T_1)^{\lambda}})$ because the local field at each site was continuously modulated by the incommensurate SDW. Since all relaxation profiles above 1.76 K in the SDW state could be fitted by the same fitting parameter, $\lambda = 0.5$, the distribution of sites is likely almost independent of temperature and T_1^{-1} corresponds to the intrinsic relaxation time. In agreement with previous experiments, T_1^{-1} diverged at T_{SDW}, and decreased in the temperature range $T^* < T < T_{SDW}$, becoming almost independent of temperature at around 5 K, as previously shown by ^{13}C NMR [6]; T_1^{-1} then sharply decreases below T^* as in ^{77}Se NMR [7]. The temperature dependence of T_1^{-1} suggested thermal activation below T^*. The activation energy below 4.2 K could be determined with an activation fitting curve as $\Delta \approx 16$ K, with an anomaly at T^* in this configuration.

To examine the details of its spectrum, we measured NMR spectra at $\theta = 113°$. Below T^*, we observed a fine structure [Fig. 3(a)], which developed as the temperature decreased. A glassy structure was observed by measuring specific heat at around 4 K, but became static below 2 K [10]. The fine structure clearly observed at 1.76 K was constructed mainly from five peaks superimposed on the IC SDW structure [Fig. 3(b)]. Since glassy behavior below 4 K suggests disorder or inhomogeneity, and the five peaks were derived from the U-shaped IC SDW spectrum, this fine structure is likely due to a commensurate SDW structure coexisting with the IC SDW structure. The intermediate state may be observed in previous ^{13}C NMR [6]. The peak observed around 85.552 MHz in our spectrum at 3.5 K

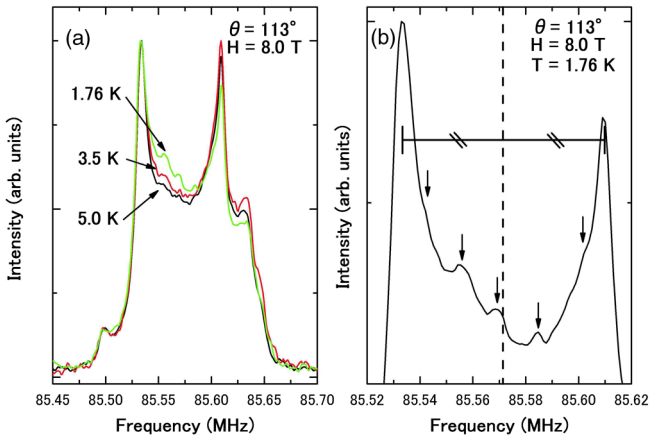

FIG. 3 (color online). (a) Temperature dependence of the NMR spectrum from 5 to 1.76 K with the magnetic field rotated 23° from the b' axis ($\theta = 113°$). (b) Fine structure of the NMR spectrum at 1.76 K in the same magnetic field direction.

apparently corresponds to the peak observed around 150 ppm at 4.2 K [6]. The shape of the SDW spectrum at 1.76 K can be expressed using the commensurate wave vector, $0.5\boldsymbol{a}^* + 0.25\boldsymbol{b}^* + 0\boldsymbol{c}^*$, close to the deduced value of the SDW from ^{1}H NMR line shape [5,22] and the satellite reflection due to the charge-density wave (CDW) from diffuse x-ray scattering [23], where $\boldsymbol{a}^*$, $\boldsymbol{b}^*$, and $\boldsymbol{c}^*$ denote the reciprocal lattice vectors.

Figure 4(a) shows a schematic view of the conducting TMTSF layer and the equiphase surface of the commensurate SDW with ordering vector (0.5 0.25 0). The open and closed circles represent two TMTSF molecules in a unit cell. The NMR shift δ_i at the ith molecule ($i = 0$–7) in the commensurate 2×4 region shown in Fig. 4(a) can be expressed as

$$\delta_i \propto \cos\Phi_i, \tag{1}$$

where Φ_i represents the phase shift on the ith cule in the 2×4 unit. The phases for two TMTSF molecules in a unit cell could be determined as

$$\Phi_i = \begin{cases} \frac{\pi i}{4} & \text{(open circle; } i = \text{even number)} \\ \frac{\pi(i-1)}{4} + \phi & \text{(closed circle; } i = \text{odd number).} \end{cases} \tag{2}$$

Here, ϕ represents the phase difference between two TMTSF molecules in a unit cell. The model of $\phi = \pi/2$ corresponds to the regular stack of TMTSF molecules. The phase modulation in a 2×4 cell is expressed as the equivalent phase modulation on a one-dimensional chain [Fig. 4(b)]. For an incommensurate SDW structure, the phase shift at the jth molecule in a one-dimensional chain can be expressed as

$$\delta_j \propto \cos(\Phi_{j\text{mod}8} + \psi_j + \theta). \tag{3}$$

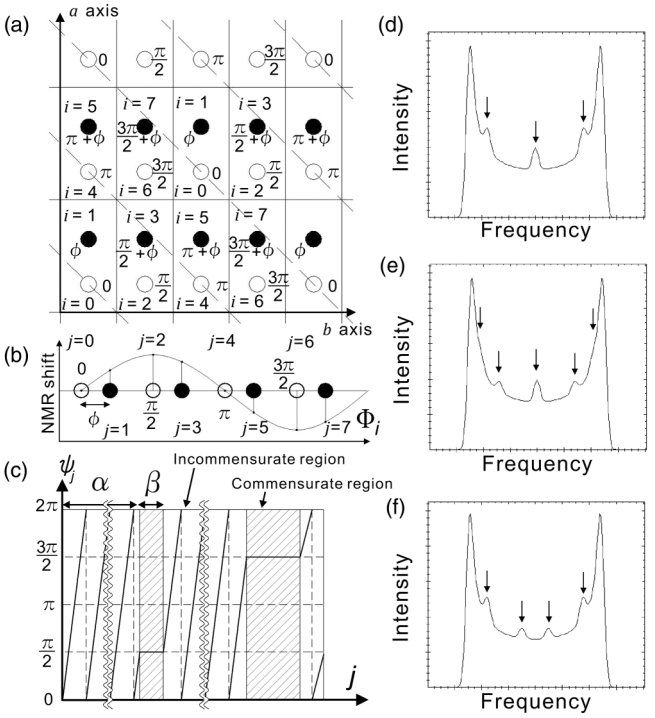

FIG. 4. (a) Schematic view of the conducting TMTSF layer, the equiphase lines of the SDW assuming the wave vector (0.5 0.25 0), and the phases at each TMTSF site. (b) NMR shift in response to the internal magnetic field at each site: ϕ is the phase difference between two TMTSF molecules in a unit cell. (c) Proposed discommensurate structure [14,15]: ψ_j is the phase shift of the SDW on each region and j is a site number in a one-dimensional chain. (d)–(f) Results of the simulation using the following constants in Eqs. (3) and (4): (d) $\phi = \pi/4$, $\theta = 0$, and $\bar{\alpha}/\bar{\beta} = 16$, (e) $\phi = 5\pi/16$, $\theta = 0$, and $\bar{\alpha}/\bar{\beta} = 16$, and (f) $\phi = 5\pi/16$, $\theta = \pi/4$, and $\bar{\alpha}/\bar{\beta} = 16$.

Here, θ denotes an initial phase constant. The symbol ψ_j is the contribution of incommensurability, which can be expressed as

$$\psi_j \propto |\Delta k| j, \tag{4}$$

where $|\Delta k|$ corresponds to the difference between commensurate and incommensurate SDW wave numbers. For an equivalent one-dimensional chain, we simulated the shape of the NMR spectrum using a partial commensurate model [Fig. 4(c)], in which the phase shift ψ_j is partially fixed to $n\pi/2$ and a commensurate SDW region is realized in the system. Figures 4(d)–4(f) show the results with several sets of parameters for the phenomenological linewidths. Since the observed fine structure is due mainly to five peaks, with the central peak located at the center of the IC SDW spectrum, the simulated spectrum with $\phi = 5\pi/16$ and $\theta = 0$ is the most suitable. The result obtained with $\phi = 5\pi/16$ corresponds to weak dimerization.

It is unclear whether such an inhomogeneous state exists above 4 K. Nuclear spin relaxation in the SDW state is due in part to thermally excited electron spin and in part to the

collective motion in the SDW state. As T_1^{-1} in the temperature range $T^* < T < T_{SDW}$ did not show behavior commensurate with thermal activation, the mechanism is thought to involve collective motion. The excitation of the phason in the IC SDW state shows a behavior indicating no or only a small phason gap due to impurities [24]. Therefore, the behavior of T_1^{-1} in the range $T^* < T < T_{SDW}$ suggests that the nuclear spin relaxation is due to the phason in the IC SDW state. In contrast, excitation of the phason in the commensurate SDW state has a gap structure [24]. The rapid decrease in T_1^{-1} below T^* may indicate the emergence of the excitation gap in the phason mode due to the development of a commensurate region. Indeed, T_1^{-1} rapidly decreased in the commensurate SDW state of $(TMTTF)_2Br$ [25]. However, the results of the simulation suggest that the volume of the incommensurate region is over 90% that of the SDW and that the profile can be almost completely determined by the incommensurate region in $(TMTSF)_2PF_6$. In the case of simple phase separation, the phason gap in the incommensurate region could not open just as above T^*. Since the phason dynamics in the incommensurate region are locked by both ends of those in the commensurate region, a gaplike behavior is expected. This gaplike behavior in the incommensurate region suggests not a simple phase separation but partial phase locking in the incommensurate SDW.

The development of commensurability provides an interpretation of the disappearance of the quantum oscillations below T^*. Apparently, the behavior of the quantum oscillations is not due to drastic changes in electronic structure caused by macroscopic phase transition but to changes in scattering. The emergence of microscopic partial commensurability at T^* may be associated with an increase in scattering rate resulting from additional umklapp scattering processes or a scattering at the microscopic incommensurate-commensurate boundary. This may be responsible for an abrupt change in the mean-free path that controls the amplitude of the quantum oscillations and may then explain their suppression at T^*.

The commensurate SDW state may compete with the mixed CDW-SDW state because both appear and disappear in the same temperature range. CDW coexisting with SDW has been observed by x rays in the range $T^* < T < T_{SDW}$ [23,26]. The mixed CDW-SDW modulation can be constructed by combining the CDWs of up and down spins:

$$\rho_\uparrow(x) = \bar{\rho} - A\sin(2k_F x - \theta_0), \quad (5)$$

$$\rho_\downarrow(x) = \bar{\rho} + A\sin(2k_F x + \theta_0), \quad (6)$$

where $\bar{\rho}$ represents the average density of each spin. A CDW corresponds to $\rho_\uparrow + \rho_\downarrow$, and a SDW corresponds to $\rho_\uparrow - \rho_\downarrow$. Phase differences θ_0 of $\pi/2$ and 0 result in a pure CDW or a pure SDW ground state, respectively [27]. The mixed CDW-SDW modulation state could be explained by a phase shift from $\theta_0 = 0$. The disappearance of CDW below T^* [23] suggests a pure SDW state. Therefore, the commensurate SDW region develops in the pure SDW ground state.

Although a previous study suggested a glasslike inhomogeneous state [10], its details were unclear. We therefore examined the magnetic profile of the inhomogeneous state by NMR spectroscopy. The commensurate magnetic structure emerged dynamically around 4 K. The dynamics slowed at the glass transition as temperature decreased, freezing below 2 K and resulting in the appearance of the inhomogeneous structure, consisting of commensurate and incommensurate regions.

The authors thank N. Matsunaga and K. Nomura of Hokkaido University for stimulating discussions. This study was supported in part by a Grant-in Aid for Scientific Research (Grant No. 18540306) and a Grant-in Aid for Young Scientists (B) (Grant No. 23740249) from the Ministry of Education, Culture, Sports, Science, and Technology of Japan.

*atkawa@phys.sci.hokudai.ac.jp

[1] D. Jérome, Science **252**, 1509 (1991).
[2] N. Thorup, G. Rindorf, H. Soling, and K. Bechgaard, Acta Crystallogr. Sect. B **37**, 1236 (1981).
[3] D. Jérome, A. Mazaud, M. Ribault, and K. Bechgaard, J. Phys. Lett. **41**, 95 (1980).
[4] P. M. Chaikin, J. Phys. I (France) **6**, 1875 (1996).
[5] T. Takahashi, Y. Maniwa, H. kawamura, and G. Saito, Physica (Amsterdam) **143B**, 417 (1986).
[6] E. Barthel, G. Quirion, P. Wzietek, D. Jérome, J. B. Christensen, M. Jørgensen, and K. Bechgaard, Europhys. Lett. **21**, 87 (1993).
[7] S. Valfells, P. Kuhns, A. Kleinhammes, J. S. Brooks, W. Moulton, S. Takasaki, J. Yamada, and H. Anzai, Phys. Rev. B **56**, 2585 (1997).
[8] K. Nomura, N. Keitoku, T. Shimizu, T. Sambongi, M. Tokumoto, N. Kinoshita, and H. Anzai, J. Phys. IV (France) **03**, C2-21 (1993).
[9] A. Hoshikawa, K. Nomura, S. Takasaki, J. Yamada, S. Nakatsuji, H. Anzai, M. Tokumoto, and N. Kinoshita, J. Phys. Soc. Jpn. **69**, 155 (2000).
[10] J. C. Lasjaunias, K. Biljaković, P. Monceau, and K. Bechgaard, Solid State Commun. **84**, 297 (1992); J. C. Lasjaunias, K. Biljaković, F. Nad', P. Monceau, and K. Bechgaard, Phys. Rev. Lett. **72**, 1283 (1994).
[11] F. Creuzet, C. Bourbonnais, L. G. Caron, D. Jérome, and A. Moradpour, Synth. Met. **19**, 277 (1987).
[12] C. Bourbonnais, P. Stein, D. Jérome, and A. Moradpour, Phys. Rev. B **33**, 7608 (1986).
[13] F. Nad', P. Monceau, and K. Bechgaard, Solid State Commun. **95**, 655 (1995).
[14] W. L. McMillan, Phys. Rev. B **14**, 1496 (1976).
[15] A. Hoshikawa, K. Nomura, S. Takasaki, J. Yamada, S. Nakatsuji, H. Anzai, M. Tokumoto, and N. Kinoshita, J. Phys. Soc. Jpn. **69**, 1457 (2000).
[16] Z. Z. Wang, H. Salva, P. Monceau, M. Renard, C. Roucau, R. Ayroles, F. Levy, L. Guemas, and et A. Meerschaut, J. Phys. Lett. **44**, 311 (1983).

[17] J. P. Ulmet, P. Auban, A. Khmou, and S. Askenazy, J. Phys. Lett. **46**, 535 (1985).
[18] J. P. Ulmet, A. Khmou, and L. Bachere, Physica (Amsterdam) **143B**, 400 (1986).
[19] S. Uji, J. S. Brooks, M. Chaparala, S. Takasaki, J. Yamada, and H. Anzai, Phys. Rev. B **55**, 12 446 (1997).
[20] J. Yamada, S. Satoki, S. Mishima, N. Akashi, K. Takahashi, N. Masuda, Y. Nishimoto, S. Takasaki, and H. Anzai, J. Org. Chem. **61**, 3987 (1996).
[21] Y. Kimura, M. Misawa, and A. Kawamoto, Phys. Rev. B **84**, 045123 (2011).
[22] J. M. Delrieu, M. Roger, Z. Toffano, E. W. Mbougue, P. Fauvel, R. S. James, and K. Bechgaard, Physica (Amsterdam) **143B**, 412 (1986).
[23] S. Kagoshima, Y. Saso, M. Maesato, R. Kondo, and T. Hasegawa, Solid State Commun. **110**, 479 (1999); S. Kagoshima, Y. Saso, M. Maesato, R. Kondo, T. Yamaguchi, V. A. Bondarenko, and T. Hasegawa, Synth. Met. **117**, 39 (2001).
[24] P. A. Lee, T. M. Rice, and P. W. Anderson, Solid State Commun. **14**, 703 (1974).
[25] S. Fujiyama and T. Nakamura, J. Phys. Chem. Solids **63**, 1259 (2002).
[26] J. P. Pouget and S. Ravy, Synth. Met. **85**, 1523 (1997).
[27] A. W. Overhauser, Phys. Rev. **167**, 691 (1968); N. Kobayashi and M. Ogata, J. Phys. Soc. Jpn. **66**, 3356 (1997).